RSC Advances

ROYAL SOCIETY OF CHEMISTRY

www.rsc.org/advances

Synthesis, Properties of Quaternary Ammonium Surfactants Containing a Methoxy Benzyl Substitute

Zhenlong Zhao, Xiangfeng Guo*, Lihua Jia*, Yanyan Liu

College of Chemistry and Chemical Engineering, Key Laboratory of Fine Chemicals of College of Heilongjiang Province, Qiqihar University, Qiqihar 161006, China.

Graphic abstract

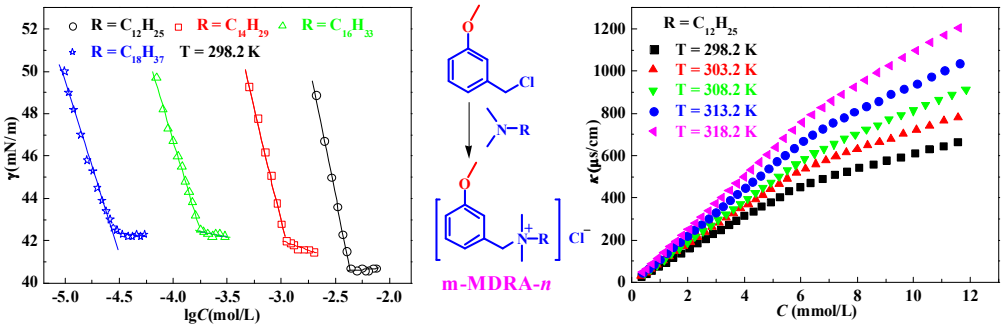

m-MDRA-*n* exhibit high surface activity, excellent adsorptive and bacterial properties, thermodynamic functions of micellization for m-MDRA-*n* were researched at different temperature.

Synthesis, Properties of Quaternary Ammonium Surfactants Containing a Methoxy Benzyl Substitute

Zhenlong Zhao, Xiangfeng Guo*, Lihua Jia*, Yanyan Liu

College of Chemistry and Chemical Engineering, Key Laboratory of Fine Chemicals of College of Heilongjiang Province, Qiqihar University, Qiqihar 161006, China.

*Corresponding author. Email: xfguo@163.com (X. Guo); jlh29@163.com (L. Jia).

Abstract A series of novel methoxybenzyl-containing quaternary ammonium surfactants, namely *N*,*N*-dimethyl-*N*-alkyl-*N*-(m-methoxybenzyl) ammonium chloride (m-MDRA-*n*), were synthesized from m-methoxybenzyl chloride and *N,N*-dimethyl-*N*-alkyl tertiary amine. The structure of those products was characterized by FT IR, ^{1}H NMR, ^{13}C NMR and MS. Their surface activity, absorption and aggregation behavior in aqueous solution at different temperature were studied by surface tension and conductivity method. The results showed that the critical micelle concentration (CMC) of m-MDRA-*n* were much lower than traditional surfactants of *N,N*-dimethyl-*N*-alky-*N*-benzyl ammonium chloride(BAC), which indicated that m-MDRA-*n* containing methoxybenzyl exhibited a higher surface activity and easier to aggregate in the aqueous solution. The standard free energy (ΔG_{mic}) and standard enthalpy (ΔH_{mic}), standard entropy (ΔS_{mic}) were studied by isothermal titration calorimetry (ITC). In addition, m-MDRA-*n* exhibited a high bactericidal activity.

Key Word: methoxybenzyl, surfactants, synthesis, surface activity, aggregation behavior, thermodynamics, bactericidal activity

Quaternary ammonium surfactants which exhibit high surface activity, excellent

adsorptive and bacterial properties have been widely applied in detergent [1], emulsification [2], phase transfer catalysis [3], materials synthesis [4, 5], separation [6], corrosion inhibitors for metal [7], sterilization [8] and so on. In order to study the relationship between structure and properties and enhance its performance of surfactants further, people designed and synthesized different kinds of novel quaternary ammonium surfactants modified with diverse functional group substituent.

Halar et al. [9] inserted the amide group into DTAB, namely dodecyl *N*-ethanamide *N,N,N*-trimethylammonium bromide, the CMC was tested by conductivity method. Compared with the DTAB, the CMC of these surfactants was found to be much lower. This could be related to the fact that the presence of amide moiety of surfactants probably facilitated the aggregation through intermolecular hydrogen bonding. Two series of long chain imidazolium and pyridinium based ionic liquids containing an ester functional group in the alkyl side chain were synthesized and their thermal stability, aggregation behavior in aqueous medium, antimicrobial activity were investigated [10]. Song et al. [11] designed and synthesized a series of surfactants containing different hydroxyl groups, it turned out that the hydrogen bonds formed by the substituted hydroxyl groups promoted surfactant adsorption at the air/water interface and aggregation in solution. The influence of acryloxyl group on surface active and self-assembly property of cationic surfactants was determined by surface tension measurement, electrical conductivity, fluorescence and dynamic light scattering measurements [12], the introduction of acryloxyl group resulted in a lower CMC value, higher degree of ionization.

As a typical cationic surfactants, *N*,*N*-dimethyl-*N*-alkyl-*N*-benzyl ammonium chlorides

(BAC) is a effective bactericidal agent. It is extensively found in pharmaceutical formulations [13], food preservatives [14], medical sterilization [15], bio-composite materials [16]. However, the influence of functional group inserting into the molecular structure on the performance of BAC still received little attention.

Hence, a methoxyl group was introduced into the meta-position of benzyl of BAC, a series of new quaternary ammonium surfactants, *N*,*N*-dimethyl-*N*-alkyl-*N*-(m-methoxy benzyl) ammonium chloride, were synthesized, which were denoted by m-MDRA-*n*. The surface activity, absorption and aggregation behavior in aqueous solution at different temperature were studied by surface tension and conductivity methods. The results show that m-MDRA-*n* exhibited excellent surface activity and absorption performance compared with BAC. In addition, m-MDRA-12 exhibited excellent bactericidal activity.

Experimental

Materials and Instruments

All reagents were analytical grade reagents without further purification during the process of synthesis. Melting point (m.p) was measured by using X-6 micro melting point apparatus, Beijing Tektronix Instrument Company; FT-IR was obtained through using Avatar-370 type infrared spectrometer, American Nicolet Company; ^{1}H NMR and ^{13}C NMR were recorded by using Avance 400 superconducting NMR, Switzerland Bruker Company, $CDCl_3$ used as the solvents; mass spectral analyses were carried out on an Agilent 6310 ESI-Ion Trop Mass spectrometer, American Agilent Company; surface tension was tested on a K10 Processor Tensionmeter, Germany Kruss Company; conductivity was measured on Alvarez DDS-307 conductivity analyzer, Shanghai Precision and Scientific Instrument

Company; isothermal titration calorimetry (ITC) experiments were performed by using the VP-ITC, American MicroCal Company.

Synthesis of m-MDRA-*n*

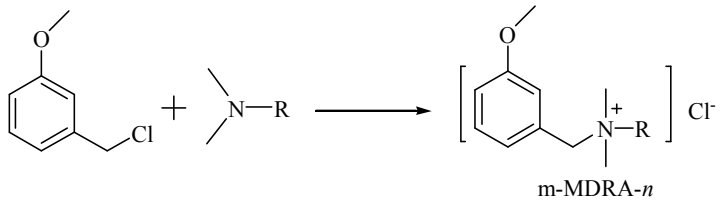

n = 12, R = $C_{12}H_{25}$; n = 14, R = $C_{14}H_{29}$; n = 16, R = $C_{16}H_{33}$; n = 18, R = $C_{18}H_{37}$

Scheme 1 Synthetic route of m-MDRA-*n*

N,*N*-dimethyl-*N*-alkyl tertiary amine with different length of carbon chain and m-methoxybenzyl chloride (molar ratio 1.2:1) were stirred in the Erlenmeyer bulb with a right amount isopropanol at reflux temperature for 12 h, respectively. Then the mixture was cooled to room temperature and removed the solvent by rotary evaporation to afford a yellowish solid. Further, the residue was purified by recrystalizing three times, which used the mixed solvent of ethyl acetate, petroleum ether and acetone. At last, the white solids were obtained, that were *N*,*N*-dimethyl-*N*-alkyl-*N*-(*m*-methoxy benzyl) ammonium chlorides, which were denoted by m-MDRA-*n*, *n*=12, 14, 16, 18, represents the length of hydrophobic group, respectively. The melting point was measured and the structure of all products was identified by FT IR, ^{1}H NMR, ^{13}C NMR and MS.

Characterization of m-MDRA-*n*

m-MDRA-12 yield: 60 %, m.p: 44.6-45.4 ^{o}C. FT IR (KBr pellet) v (cm^{-1}): 2921 (C–H stretching, methyl), 2856 (C–H stretching, methylene), 1597, 1491 (C=C stretching, benzene ring), 1176 (C–N stretching), 1262, 1042 (C–O–C stretching), 600–900 (C–H, aromatic hydrocarbon). ^{1}H NMR ($CDCl_3$, 600 MHz): δ 7.36 (t, J = 7.8 Hz, 1H, , Ar*H*), 7.25

(d, *J* = 8.4 Hz, 1H, , Ar*H*), 7.18 (d, *J* = 7.2 Hz, 1H, Ar*H*), 7.01 (dd, *J* = 1.8 Hz, 1.8 Hz, 1H, Ar*H*), 4.98 (s, 2H, CH_2N), 3.84 (s, 3H, COCH_3), 3.51-3.48 (t, *J* = 7.8 Hz, 2H, NCH_2(CH_2)$_{10}$$CH_3$), 3.32 (s, 6H, 2C$H_3$N), 1.79 (s, 2H, NCH_2CH_2(CH_2)$_9$$CH_3$), 1.35-1.25 (m, 18H, NCH_2CH_2(CH_2)$_9$$CH_3$), 0.88 (t, *J* = 6.6 Hz, 3H, N(CH_2)$_{11}$CH_3). ^{13}C NMR(150 MHz, CD_3Cl) δ(*10-6):161.38, 131.58, 130.20, 126.66, 120.17, 117.70, 68.79, 65.18, 57.05, 51.29, 33.30, 30.97, 30.85, 30.78, 30.72, 30.67, 27.74, 24.36, 24.08, 15.52. ESI MS (m/z): [M－Cl]$^+$ 333.4.

m-MDRA-14 yield: 82 %, m.p: 47.3-48.0 ^{o}C. FT IR(KBr pellet) *v* cm^{-1}: 2917 (C–H stretching, methyl), 2851 (C–H stretching, methylene), 1601, 1487 (C=C stretching, benzene ring), 1172（C–N stretching), 1270, 1041 (C–O–C stretching), 800–900 (C–H, aromatic hydrocarbon). ^{1}H NMR ($CDCl_3$, 600 MHz): δ 7.36 (t, *J* = 7.8 Hz, 1H, , Ar*H*), 7.25 (d, *J* = 8.4 Hz, 1H, , Ar*H*), 7.18 (d, *J* = 7.2 Hz, 1H, Ar*H*), 7.01 (dd, *J* = 1.8 Hz, 1.8 Hz, 1H, Ar*H*), 4.98 (s, 2H, CH_2N), 3.84 (s, 3H, COCH_3), 3.51-3.48 (t, *J* = 7.8 Hz, 2H, NCH_2(CH_2)$_{10}$$CH_3$), 3.32 (s, 6H, 2C$H_3$N), 1.79 (s, 2H, NCH_2CH_2(CH_2)$_9$$CH_3$), 1.35-1.25 (m, 22H, NCH_2CH_2(CH_2)$_{11}$$CH_3$), 0.88 (t, *J* = 6.6 Hz, 3H, N(CH_2)$_{11}$CH_3). ^{13}C NMR(150 MHz, CD_3Cl) δ(*10-6):161.39, 131.58, 130.18, 126.65, 120.06, 117.72, 68.80, 65.19, 57.05, 51.30, 33.32, 31.08, 31.04, 30.98, 30.86, 30.79, 30.76, 30.68, 27.74, 24.36, 24.09, 15.53. ESI MS (m/z): [M－Cl]$^+$ 362.4.

m-MDRA-16 yield: 83 %, m.p: 51.8-53.1 ^{o}C. FT IR(KBr pellet) *v* cm^{-1}: 2921 (C–H stretching, methyl), 2852 (C–H stretching, methylene), 1597, 1495 (C=C stretching, benzene ring), 1172（C–N stretching), 1262, 1037 (C–O–C stretching), 800–900 (C–H, aromatic hydrocarbon). ^{1}H NMR ($CDCl_3$, 600 MHz): δ 7.36 (t, *J* = 7.8 Hz, 1H, , Ar*H*), 7.25

(d, *J* = 8.4 Hz, 1H, Ar*H*), 7.18 (d, *J* = 7.2 Hz, 1H, Ar*H*), 7.01 (dd, *J* = 1.8 Hz, 1.8 Hz, 1H, Ar*H*), 4.98 (s, 2H, CH_2N), 3.84 (s, 3H, COCH_3), 3.51-3.48 (t, *J* = 7.8 Hz, 2H, NCH_2(CH_2)$_{10}$$CH_3$), 3.32 (s, 6H, 2C$H_3$N), 1.79 (s, 2H, NCH_2CH_2(CH_2)$_9$$CH_3$), 1.35-1.25 (m, 26H, NCH_2CH_2(CH_2)$_{13}$$CH_3$), 0.88 (t, *J* = 6.6 Hz, 3H, N(CH_2)$_{11}$CH_3). ^{13}C NMR(150 MHz, CD_3Cl) δ(*10-6):161.38, 131.57, 130.19, 126.65, 120.06, 117.71, 68.81, 65.16, 57.05, 51.31, 33.33, 31.10, 31.06, 31.05, 30.99, 30.86, 30.80, 30.76, 30.68, 27.74, 24.36, 24.09, 15.52. ESI MS (m/z): $[M-Cl]^+$ 390.5.

m-MDRA-18 yield: 95 %, m.p: 58.6-60.5 °C. FT IR(KBr pellet) *v* cm^{-1}: 2921 (C–H stretching, methyl), 2848 (C–H stretching, methylene), 1601, 1487 (C=C stretching, benzene ring), 1164 （C–N stretching), 1266, 1046 (C–O–C stretching), 800–900 (C–H, aromatic hydrocarbon). ^{1}H NMR ($CDCl_3$, 600 MHz): δ 7.36 (t, *J* = 7.8 Hz, 1H, , Ar*H*), 7.25 (d, *J* = 8.4 Hz, 1H, Ar*H*), 7.18 (d, *J* = 7.2 Hz, 1H, Ar*H*), 7.01 (dd, *J* = 1.8 Hz, 1.8 Hz, 1H, Ar*H*), 4.98 (s, 2H, CH_2N), 3.84 (s, 3H, COCH_3), 3.51-3.48 (t, *J* = 7.8 Hz, 2H, NCH_2(CH_2)$_{10}$$CH_3$), 3.32 (s, 6H, 2C$H_3$N), 1.79 (s, 2H, NCH_2CH_2(CH_2)$_9$$CH_3$), 1.35-1.25 (m, 30H, NCH_2CH_2(CH_2)$_{15}$$CH_3$), 0.88 (t, *J* = 6.6 Hz, 3H, N(CH_2)$_{11}$CH_3). ^{13}C NMR(150 MHz, CD_3Cl) δ(*10-6):161.40, 131.59, 130.17, 126.65, 120.05, 117.74, 68.80, 65.20, 57.05, 51.30, 33.33, 31.12, 31.10, 31.07, 31.06, 30.99, 30.87, 30.79, 30.77, 30.68, 27.74, 24.37, 24.10, 15.53. ESI MS (m/z): $[M-Cl]^+$ 418.0.

Surface Tension

The surface tension measurements of aqueous solutions were conducted by the ring method using a Kruss K10 tensiometer with a platinum ring. The platinum ring was cleaned by the ultrapure water and flamed to drying before each measurement. The tested

temperature was controlled at 298.2 K within ±0.1 K. At least three measurements were taken for each solution. Surface tension was considered to be equilibrium when the standard deviation of three consecutive measurements did not exceed 0.10 mN/m.

Conductivity

Conductivity was measured on DDS 307 digital conductivity meter with DJS-1C electrode (cell constant K=1 cm^{-1}) at different temperature. The solutions of individual surfactants with known concentration were prepared, then the solutions were progressively diluted and the specific conductivity values were measured. The conductivity of ultra-pure water was below 6.8×10^{-7} $S\cdot cm^{-1}$.

Isothermal titration calorimetry (ITC)

The ITC experiments were performed by using the VP-ITC calorimeter, which has the precision of 0.5 ncal s^{-1}. The calorimeter has a sample cell with the fixed volume of 1.4008 mL. The sample cell was filled with degassed ultrapure water. The surfactant solution (the concentration is about ten times of CMC) was injected into sample cell in 29 portions of 10 μL using a spinning syringe (maximum volume of 290 μL). The ITC experiments were carried out at 298.2 K.

Bactericidal Activity

The antimicrobial activity of m-MDRA-*n* was tested according to Chinese standard GB15981–1995, respectively. The nutrient agar plates (pH=7.2–7.4) were prepared after sterilizing under 121^{o}C for 30 min. The density of bacterial suspension, including *Staphyloccocus aureus*, *Streptococcus, Escherichia coli and Salmonella*, was $5\times10^{5}\sim5\times10^{6}$ cfu/mL, respectively. The aqueous solution of m-MDRA-*n* of different concentration was

transferred into a test tube and placed in the thermostat water bath (20 ^{o}C), respectively. Then the bacterial suspension was added into the tube, after 30 min the neutralizer (1 % lecithin) was put into the mixing solution, 10 min later the amount of viable bacteria was noted by the colony count method. The concentration of the surfactant with sterilizing rate over 99.9% was picked up as minimum bactericidal concentration (MBC) [17]. Every experiment was repeated three times.

Results and discussion

Surface activity

The curves of surface tension *vs*. log molar concentration (lg*C*) of m-MDRA-*n* aqueous solutions at 298.2 K were shown in Figure 1. The values of CMC were determined as the crossing point of the two straight linear portions in the surface tension plots [18].

Fig. 1

As expected, increasing the concentration of surfactants (*C*), the surface tension (γ) decreased until the breaking point appeared. The CMC and γ at CMC (γ_{CMC}) were obtained from the curves of γ-lg*C* as given in Table 1. It was found the CMC values of m-MDRA-*n* were lower than that of the corresponding BAC-*n* with the same alky chain, which indicated the m-MDRA-*n* were easier to form the micelles in the aqueous solution compared to BAC-*n*.

Tab. 1

The relationship between CMC and the tail length of hydrophobic group followed Stauff–Klevens equation for linear single-chain amphiphiles [19], as shown in equation (1).

$$\lg CMC = A - Bx \quad (1)$$

A and B are empirical constant in the equation (1), the constant A represents the influence of the polar group on micelle formation. The greater the value of A is, the weaker the ability of micelle formation is. The constant B stands for the effect of each additional methine of the hydrophobic group on the average contribution of the ability to forming micelles; *x* is the number of carbon atoms in the hydrocarbon chain.

Fig. 2

The relation of log CMC *vs*. alkyl tail length (*x*) was shown in Figure 2. The values of A and B could be found from Figure 2 according to the equation (1). The values of A were 2.036 and 2.421 for m-MDRA-*n* and BAC-*n*, respectively. It was obviously that the former was significantly less than the later, which demonstrated that the ability of forming micelles of m-MDRA-*n* in aqueous solution was stronger than that of BAC-*n*. The methoxyl inserting to the head groups of m-MDRA-*n* led to increasing the dimension of head group and the spatial effect on the forming micelle increased. On the other side, the introduction of methoxyl made the surface charge well dispersed on the entire head group [20], thereby reducing the surface charge density of head groups and the electrostatic repulsion among the head groups, however, the influence of the spatial effect was less than that of the electrostatic repulsion of m-MDRA-*n* on the forming micelle, for the methoxyl group was

not a huge group. In addition, methoxyl group as an electron-donating group could weaken the electropositive of cationic nitrogen atom, likewise achieving the reduction of electrostatic repulsion, so the ability of forming micelles of m-MDRA-*n* was promoted by introducing methoxyl group. Both of B was almost same for m-MDRA-*n* and BAC-*n*, which mean that it was negligible for the effect of inserting methoxyl group to the head group on the hydrophobicity of m-MDRA-*n* compared with that of BAC-*n*.

The maximum adsorbed amount of surfactant (Γ_{max}) and the average minimum area per surfactant molecule (A_{min}) can be calculated according to the Gibbs adsorption isotherm equations (2), (3) [21, 22].

$$\Gamma_{max} = -\left(\frac{1}{2.303nRT}\right)\left(\frac{\partial\gamma}{\partial \lg C}\right)_T \quad (2)$$

$$A_{min} = \frac{1}{\Gamma_{max} N_A} \quad (3)$$

Where γ is the surface tension in mN/m, C represents the concentration of surfactant (mol/L), R is equal to 8.314 ($J \cdot mol^{-1} \cdot K^{-1}$), T is the absolute temperature (K), $\frac{\partial\gamma}{\partial \lg C}$ is the slope of a corresponding oblique line. Γ_{max} is the saturated adsorption ($\mu mol/m^2$), N_A is Avogadro's constant, A_{min} is the average area per molecule occupied at the air/water interface (nm^2), n is the number of ionic species whose concentration at the interface varies with the surfactant concentration in solution, it is assumed to be 2 for the ionic surfactant. The surface and adsorption parameters were summarized in Table 1.

According to the literature [23], the hydrophobic interactions could be reinforced between the molecules with the increase of chain length, attributed to an enhancement of the hydrophobic character, which favors the orderly assembly of the surfactants at the interface, resulting in a decreasing of the A_{min} values. Whereas, the average area per

molecule (A_{min}) of m-MDRA-*n* increased in our study, and the saturated adsorption (Γ_{max}) decreased with increasing the length of hydrophobic carbon chain from 12 up to 18. The possible explanation was that the longer alkyl chain of amphiphilic molecules had a more prone to curl, resulting in an amplification on average area per molecule [24].

Conductivity

The curves of conductivity (κ) *vs.* concentration (C) of m-MDRA-*n* at different temperature were shown in Figure 3. The values of CMC were taken as the intersection of two straight linar portions with different slopes [25]. The degree of ionization of the micelles (α) were acquired from the ratio of the slopes while the degree of counterion binding (β) can be calculated from β=1–α. The CMC and β were listed in Table 2.

The values of CMC of m-MDRA-*n* obtained from conductivity were closed to that of derived from surface tension method. It is interested that the plots of m-MDRA-18 showed a slight curvature toward the *y* axis past CMC, however, the common surfactants had the trend to *x* axis just like m-MDRA-16, m-MDRA-14, m-MDRA-12. One reasonable explanation is that the aggregates of m-MDRA-18 exhibited the properties of premicellar which can diffuse and migrate faster in the solution. So the conductivity became higher after the formation of aggregates [20, 26]. Another possibility is that the degree of ionization of micelles of is too high for m-MDRA-18 and the conductivity method is not suitable to evidence the micellization.

The values of CMC increased with the rising of temperature for m-MDRA-*n*, it resulted from that a higher temperature would destroy the structure of water surrounding the hydrophobic group, impeding the formation of micelle [27].

Fig. 3

Tab. 2

It was of great significance to concentrate on the degree of counterion binding for the comprehension of aggregation behavior of micelles in solution. As expected that increasing the length of hydrophobic carbon chain, the values of β of m-MDRA-*n* reduced gradually. Additionally, increasing the temperature the β of m-MDRA-*n* had a trend to decrease, which illustrated the bonding of counterions to the micelles was an exothermic process, which seemed to be a reasonable picture that the counterion binding was caused by an electrostatic interaction between opposite charges [28].

The value of β of m-MDRA-12 was lower than that of the corresponding BAC-12 at 298.2 K. The existence of a methoxyl group in the head group diminished the surface charge density of m-MDRA-12, reducing the force of repulsion among the amphiphilic molecules, resulting in a closely arrangement when micelles formed. Hence, the size of micellar aggregations got smaller, the amount of positive charge became fewer on the surface of micelles, therefore the degree of counterion binding for micelles decreased.

Thermodynamic functions of micellization

The thermodynamic functions of micelle formation per mole of monomer are of great significance to discuss the micellization mechanism and contribute to a deeper understanding for amphiphiles aggregation phenomena. The CMC value is taken from the breaking point of enthalpy *vs* concentration curve (Figure 4B), corresponding to the onset of

micelle formation [29], the CMC of m-MDRA-*n* are summarized in Table 3.

The enthalpy change (ΔH_{mic}) values are obtained from ITC data. A typical illustration [30] is that the enthalpogram (Figure 4A) can be subdivided into two concentration ranges where the reaction enthalpies are almost constant. In the first concentration ranges, the final concentrations in the sample cell are below the CMC. Here, the large enthalpic effects observed are due to dilution of micelles, the demicellization process, and dilution of the resultant monomers. The sharp decrease in the reaction enthalpy curve indicates that the CMC in the sample cell has been reached. If more micellar solution is added, the micelles are no longer dissolved and the only heat caused by dilution of micelles is measured and this is the second concentration range. These integrations of each peak area (Figure 4A) give rise to the sigmoid curve in Figure 4B, i.e. the curve of calorimetric enthalpy (ΔH_{cal}) *vs* surfactant concentration. The enthalpy change (ΔH_{mic}) is obtained from the differences between the levels of the two asymptotes in the sigmoidal curve by fitting with Sigmoidal-Boltzmann equation [31], namely $\Delta H_{mic} = \Delta H_{d(f)} - \Delta H_{d(i)}$, $\Delta H_{d(f)}$ is the final height of the enthalpy of dilution of the micellar solution and $\Delta H_{d(i)}$ is the initial height including pertaining to micellar dilution, demicellization, the results are listed in Table 3.

Applying the phase separation model, the free energy and entropy change of micellization can be calculated from the following equations [32-34].

$$\Delta G_{mic} = RT \ln X_{CMC} \tag{4}$$

$$\Delta S_{mic} = \frac{\Delta H_{mic} - \Delta G_{mic}}{T} \tag{5}$$

where X_{CMC} is the surfactant molar fraction at CMC. The thermodynamic functions of micellization are summarized in Table 3.

Fig. 4

Tab.3

An expected, the values of standard free energy (ΔG_{mic}) are negative for m-MDRA-*n*, which illustrated that the formation of micelles is thermodynamically spontaneous process. The values of enthalpy change (ΔH_{mic}) for m-MDRA-*n* are negative, too. The enthalpy change mainly includes two opposing aspects during the micellization process for the surfactants. One is the removal of water molecules from around the monomeric hydrocarbon chain, and this process is endothermic; another is the transfer of the hydrocarbon chain from the water to the oil-like interior of the micelle and the transfer process is exothermic [35]. At a relative low temperature, the first process is dominated and the enthalpy change is positive; at a relative high temperature, the removal of the water term will become less significant as water becomes a more "normal" liquid and the amount of ordered water molecules around the hydrophobic alky chains decreases, the second process plays an important role during the micellization and the enthalpy change becomes more negative [36]. At a given the experiment temperature, the enthalpy change is related to the pH of solution, G. Lazzara et al. [37] studied thermodynamics of the copolymer $[(EO)_{57}(PO)_{21}]_2$ $NCH_2CH_2N[(PO)_{21}(EO)_{57}]$ (T1170) and $[(PO)_{17}(EO)_{19}]_2$ NCH_2 $CH_2N[$ $(EO)_{19}(PO)_{17}]$ (T90R4) of the acid/base equilibrium by ITC method, it is found that the enthalpy change ΔH_M slightly decreases ranging the pH from 7.9 to 2.7 due to the presence of large amount of water molecule hydrating the charged groups.

The negative values of enthalpy change of m-MDRA-*n* indicate that the transfer of the hydrocarbon chain from the water to micelle is predominant process during the micellization

compared with the removal of water molecules from around the monomeric hydrocarbon chain. Meanwhile, the introduction of a methoxy substituent to the headgroup may make a contribution to the negative value of ΔH_{mic}. The contribution of $-T\Delta S_{\mathrm{mic}}$ to ΔG_{mic} is greater than ΔH_{mic} at 298.2 K, it revealed the micellization process is driven by the entropic contribution.

With the increase of hydrophobic chain length from 12 to 18, the values of ΔH_{mic} become more and more negative, which resulted from the stronger hydrophobic interaction between the hydrophobic groups along with the length of the alkyl chain [38]. Whereas the values of ΔS_{mic} increased with raising the length of hydrophobic chain, attributed to the consequence of the increase in the amount of ordered water surrounding the alky chain [39].

Bactericidal Activity

The MBC of m-MDRA-*n* against *Staphyloccocus aureus, Streptococcus, Salmonella, Escherichia coli* were listed in Table 4.

Tab. 4

The compounds of m-MDRA-12 and m-MDRA-18 exhibited a wide antibacterial spectrum and more effective against microorganism, compared with m-MDRA-14 and m-MDRA-16. The bactericidal activities depended on the hydrophobic moieties and electron-donating groups [40], such as methoxyl group. When the number of carbon atom in alkyl chain was not enough, the electron-donating effect played a critical role in antibacterial performance, so m-MDRA-12 showed a higher bactericidal activity. However, while the number of carbon atom in alkyl chain reached to 18, the hydrophobicity of

m-MDRA-18 acted an important part in the inhibitory activity.

The bactericidal activity of m-MDRA-12 was superior to BAC-12, which revealed the introduction of methoxyl group enhanced the antimicrobial activity. The microorganism had the drug-resistance for BAC-12 which was a long-term used medical disinfectant, however, m-MDRA-12 used as a new drug for the microorganism, the bacteria had no resistance for it, so m-MDRA-12 exhibited an excellent antibacterial activity.

Conclusion

In this study, the novel methoxybenzyl-containing quaternary ammonium surfactants, m-MDRA-*n*, were synthesized by one-spot method. The effect of methoxyl on the surface activity, thermodynamic functions of micellization and bactericidal activity of m-MDRA-*n* were researched. The methoxyl-inserted m-MDRA-*n* possessed lower critical micelle concentration and stronger ability to forming micelles in aqueous solution. The values of CMC and β of m-MDRA-*n* reduced, the values of ΔH_{mic} became more negative yet the values of ΔH_{mic} increased along with the growth of alkyl chain. And increasing the temperature, the values of CMC enlarged and the degree of counterion binding (β) had a trend to decrease. Moreover, the bactericidal activity of m-MDRA-12 is superior to BAC-12, and m-MDRA-12 would serve for potential application as a new sterilizing agent.

Acknowledgements

This work was supported by the National Natural Science Foundation of China (21176125), the Natural Science Foundation of Heilongjiang Province (B201114, B201314, B201419, GC04A408-2), and the Science Research Project of the Ministry of Education of Heilongjiang Province of China (2012TD012, 12511Z030, 12521594).

References

[1] Z.H. Asadov, R.A. Rahimov, G.A. Ahmadova, K.A. Mammadova, J. Surfactants Deterg. 15 (2012) 721.

[2] A.F. Naves, R.R. Palombo, L.D.M. Carrasco, A.M. Carmona-Ribeiro, Langmuir 29 (2013) 9677.

[3] H.-Y. Wang, J.-X. Zhang, D.-D. Cao, G. Zhao, ACS Catalysis 3 (2013) 2218.

[4] M. Salajková, L.A. Berglund, Q. Zhou, J. Mater. Chem. 22 (2012) 19798.

[5] X. Ye, L. Jin, H. Caglayan, J. Chen, G. Xing, C. Zheng, V. Doan-Nguyen, Y. Kang, N. Engheta, C.R. Kagan, ACS nano 6 (2012) 2804.

[6] W. Guo, Y. Hou, W. Wu, S. Ren, S. Tian, K.N. Marsh, Green Chem. 15 (2012) 226.

[7] M.A. Hegazy, M. Abdallah, M.K. Awad, M. Rezk, Corros. Sci. 81 (2014) 54.

[8] B.P. Mowery, A.H. Lindner, B. Weisblum, S.S. Stahl, S.H. Gellman, J. Am. Chem. Soc. 131 (2009) 9735.

[9] J. Hoque, P. Kumar, V.K. Aswal, J. Haldar, J. Phys. Chem. B 116 (2012) 9718.

[10] M.T. Garcia, I. Ribosa, L. Perez, A. Manresa, F. Comelles, Langmuir 29 (2013) 2536.

[11] B. Song, S. Shang, Z. Song, J. Colloid Interface Sci. 382 (2012) 53.

[12] R. Li, F. Yan, J. Zhang, C. Xu, J. Wang, Colloids Surf., A 444 (2014) 276.

[13] C.K. Hesje, S.D. Borsos, J.M. Blondeau, J. Ocul. Pharmacol. Ther. 25 (2009) 329.

[14] S.P. Epstein, D. Chen, P.A. Asbell, J. Ocul. Pharmacol. Ther. 25 (2009) 415.

[15] M.J. Ford, L.W. Tetler, J. White, D. Rimmer, J. Chromatogr. A 952 (2002) 165.

[16] K. Liu, X. Lin, L. Chen, L. Huang, S. Cao, H. Wang, J. Agric. Food. Chem. 61 (2013) 6562.

[17] K.L. Bailey, F. Tilton, D.P. Jansik, S.J. Ergas, M.J. Marshall, A.L. Miracle, D.M. Wellman, Ecotoxicol. Environ. Saf. 80 (2012) 195.

[18] Y.-P. Zhu, A. Masuyama, Y. Kobata, Y. Nakatsuji, M. Okahara, M.J. Rose, J. Colloid Interface Sci. 158 (1993) 40.

[19] H. Klevens, J. Am. Oil Chem. Soc. 30 (1953) 74.

[20] P. Quagliotto, G. Viscardi, C. Barolo, D. D'Angelo, E. Barni, C. Compari, E. Duce, E. Fisicaro, J. Org. Chem. 70 (2005) 9857.

[21] E. Alami, G. Beinert, P. Marie, R. Zana, Langmuir 9 (1993) 1465.

[22] S. Nave, J. Eastoe, J. Penfold, Langmuir 16 (2000) 8733.

[23] T.H.V. Ngo, C. Damas, R. Naejus, R. Coudert, J. Colloid Interface Sci. 389 (2013) 157.

[24] L. Zhou, X. Jiang, Y. Li, Z. Chen, X. Hu, Langmuir 23 (2007) 11404.

[25] R. Zana, J. Colloid Interface Sci. 78 (1980) 330.

[26] A. Pinazo, X. Wen, L. Pérez, M.-R. Infante, E.I. Franses, Langmuir 15 (1999) 3134.

[27] Y. Song, Q. Li, Y. Li, L. Zhi, Colloids Surf., A 417 (2013) 236.

[28] T. Inoue, H. Ebina, B. Dong, L. Zheng, J. Colloid Interface Sci. 314 (2007) 236.

[29] G. Bai, A. Lopes, M. Bastos, J. Chem. Thermodynamics 40 (2008) 1509.

[30] S. Paula, W. Sues, J. Tuchtenhagen, A. Blume, J Phys Chem 99 (1995) 11742.

[31] S. Hait, S. Moulik, R. Palepu, Langmuir 18 (2002) 2471.

[32] M.G. D'Andrea, C.C. Domingues, S.V. Malheiros, F.G. Neto, L.R. Barbosa, R. Itri, F.C. Almeida, E. de Paula, M.L. Bianconi, Langmuir 27 (2011) 8248.

[33] R. Zana, Langmuir 12 (1996) 1208.

[34] G. Cavallaro, G. Lazzara, S. Milioto, Soft Matter 8 (2012) 3627.

[35] M.S. Ramadan, D.F. Evans, R. Lumry, J. Phys. Chem. 87 (1983) 4538.

[36] A.B. Páhi, Z. Király, Á. Mastalir, J. Dudás, S. Puskás, Á. Vágó, J. Phys. Chem. B 112 (2008) 15320.

[37] R. De Lisi, G. Giammona, G. Lazzara, S. Milioto, J. Colloid. Interface. Sci 354 (2011) 749.

[38] W. Tong, Q. Zheng, S. Shao, Q. Lei, W. Fang, J. Chem. Eng. Data 55 (2010) 3766.

[39] Z. Fan, W. Tong, Q. Zheng, Q. Lei, W. Fang, J. Chem. Eng. Data 58 (2013) 334.

[40] K. Okazaki, T. Maeda, H. Nagamune, Y. Manabe, H. Kourai, Chem. Pharm. Bull. 45 (1997) 1970.

Fig. 1 Curves of surface tension (γ) *vs*. lg *C* of m-MDRA-*n*. A: m-MDRA-12, B: m-MDRA-14, C: m-MDRA-16, D: m-MDRA-18, T = 298.2 K.

Fig. 2 Curves of log CMC *vs*. alkyl tail length.

Fig. 3 Curves of the conductivity (κ) vs. concentration of m-MDRA-*n* at 298.2 K, 303.2 K, 308.2 K, 313.2 K, 318.2 K.

Fig. 4 (A) Calorimetric traces for m-MDRA-14 at 298.2 K (heat flow against time); (B) Microcalorimetric determination ΔH_{mic} by the SBE fitting for m-MDRA-14 at 298.2 K. $\Delta H_{mic} = \Delta H_{d(f)} — \Delta H_{d(i)}$, the values of $\Delta H_{d(f)}$ and $\Delta H_{d(i)}$ are displayed directly from SBE fitting results. The CMC value is taken from the breaking point.

Fig. 1

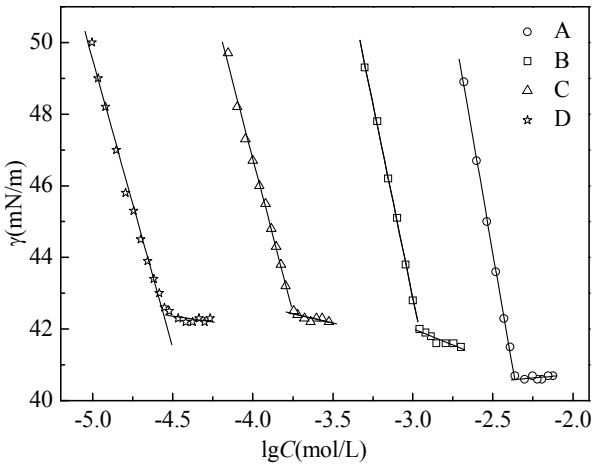

Fig. 2

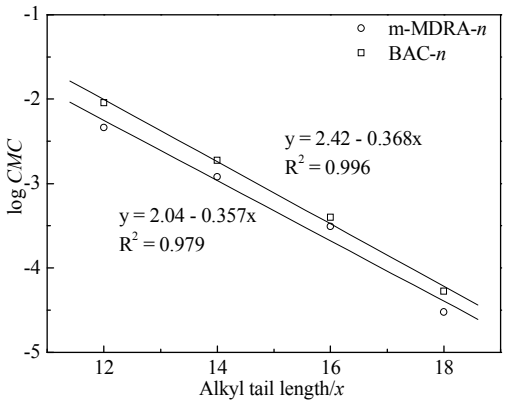

Fig.3

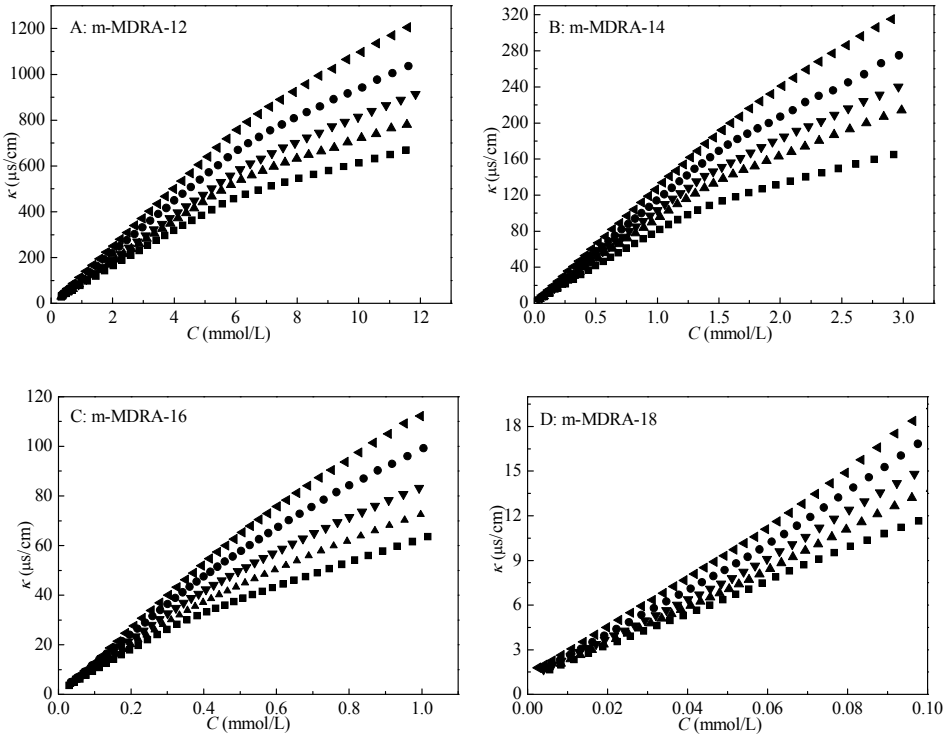

Fig.4

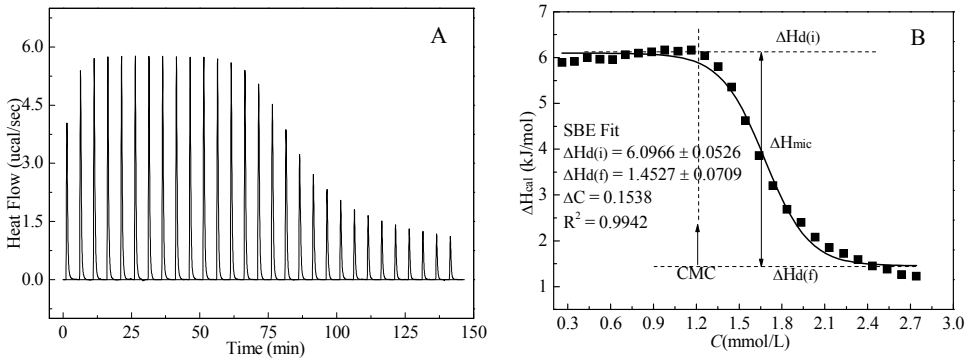

Tab. 1 Surface and adsorption parameters of m-MDRA-*n* and BAC-*n*

Tab. 2 The values of CMC, β from conductivity at different temperature

Tab. 3 The values of CMC and thermodynamic functions of micellization of m-MDRA-*n* from ITC method

Tab. 4 MBC of m-MDRA-*n*

Tab. 1

SAA	T(K)	CMC (mmol/L)	γ_{CMC} (mN/m)	Γ_{max} (μmol/m^2)	A_{min} (nm^2)	pC_{20} (mol/L)
m-MDRA-12	298	4.60	40.7	2.14	0.780	2.82
m-MDRA-14	298	1.20	41.8	1.77	0.940	3.44
m-MDRA-16	298	0.310	42.1	1.50	1.10	4.30
m-MDRA-18	298	0.0316	42.5	1.25	1.33	5.34
BAC-12	298	9.08	38.0	1.64	1.01	2.85
BAC-14	298	1.88	39.2	1.59	1.05	3.37
BAC-16	298	0.398	39.6	1.46	1.14	4.13
BAC-18	298	0.0530	40.3	1.23	1.35	5.14

Tab. 2

SAA	*m-MDRA-12*					*m-MDRA-14*				
T (K)	298.2	303.2	308.2	313.2	318.2	298.2	303.2	308.2	313.2	318.2
CMC (mmol/L)	5.91	6.16	6.25	6.32	6.64	1.36	1.41	1.44	1.48	1.57
β	0.522	0.505	0.433	0.424	0.372	0.520	0.433	0.393	0.371	0.293

SAA	m-MDRA-16					m-MDRA-18	BAC-12
T (K)	298.2	303.2	308.2	313.2	318.2	298.2	298.2
CMC (mmol/L)	0.324	0.351	0.406	0.434	0.451	0.032	9.51
β	0.355	0.299	0.286	0.230	0.215		0.587

Tab. 3

SAA	*T* *(K)*	*CMC* *(mmol/L)*	ΔG_{mic} *(kJ/mol)*	ΔH_{mic} *(kJ/mol)*	ΔS_{mic} *(J/mol·K)*	$-T\Delta S_{mic}$ *(kJ/mol)*
m-MDRA-12	298.2	4.52	-23.3	-1.86 ± 0.14	71.8	21.4
m-MDRA-14	298.2	1.26	-38.0	-4.64 ± 0.12	112	-33.4
m-MDRA-16	298.2	0.236	-42.7	-8.95 ± 0.21	113	-33.8
m-MDRA-18	298.2	0.0259	-49.5	-10.8 ± 0.2	130	38.7

Tab. 4

Samples (μg/mL)	*Staphylococcus aureus*	*Streptococcus*	*Salmonella*	*Escherichia coli*
BAC-12	97.6	195	48.8	195
m-MDRA-12	24.4	24.4	48.8	48.8
m-MDRA-14	97.6	195	195	195
m-MDRA-16	48.8	48.8	195	195
m-MDRA-18	48.8	24.4	24.4	48.8